Toroidal drift mode structure revisited: A model for small ELM regimes

H.R. Wilson[1], D. Dickinson[1,2] and C.M. Roach[2]

[1]*York Plasma Institute, Dept. of Physics, University of York, Heslington York YO10 5DD, UK*

[2]*EURATOM/CCFE Fusion Association, Culham Science Centre, Abingdon, Oxon OX14 3DB*

We review the two generic types of toroidal instabilities: *isolated* modes are the most unstable and balloon on the outboard side of the tokamak, but can only exist at certain special locations in the plasma; *general* modes, which balloon away from the mid-plane, are more stable but exist at most rational surfaces in the plasma [1]. Based on these results, we propose a new idea for small ELMs, where the crash is triggered by the sudden onset of a deeply unstable isolated mode in a pedestal where gradients are at the general mode stability boundary.

We first introduce our model 2D eigenmode equation for the electrostatic potential, ϕ, which describes toroidal drift waves and ion temperature gradient, ITG, modes [2]:

$$\left[\rho_i^2\frac{\partial^2}{\partial x^2}-\frac{\sigma^2}{\omega^2}\left(\frac{\partial}{\partial\theta}+ik_\theta sx\right)^2-\frac{2\varepsilon_n}{\omega}\left(\cos\theta+\frac{i\sin\theta}{k_\theta}\frac{\partial}{\partial x}\right)-\frac{\omega-1}{\omega+\eta_i}-k_\theta^2\rho_i^2\right]\phi(x,\theta)=0 \qquad (1)$$

This model assumes adiabatic electrons and expands the ion response for small ion Larmor radius, ρ_i, and small drifts compared to the mode frequency, ω (normalised to the electron diamagnetic frequency). The coordinates are poloidal angle, θ, and radial distance from a reference mode rational surface, x, with k_θ denoting the poloidal wavenumber. Equilibrium parameters, which depend only on x, are magnetic shear s, $\sigma=\varepsilon_n/(qk_\theta\rho_i)$, $\varepsilon_n=L_n/R$, L_n is the density scale length, R is the major radius and $\eta_i>>1$ is the ratio of density to temperature scale lengths. η_i provides the drive for the ITG mode that we shall focus on here.

A standard approach to solve Eq (1) is to employ the ballooning transformation [3]:

$$\phi(x,\theta)=\sum_m e^{-im\theta}\int_{-\infty}^{\infty}e^{im\eta}e^{-inq'x(\eta-\theta_0)}\hat{A}(x)\xi(\eta,\theta_0)d\eta \qquad (2)$$

The leading order in a large toroidal mode number, n, expansion yields the well-known ballooning equation for ξ and the leading order eigenvalue, $\omega_0(x,\theta_0)$:

$$\left[\frac{\sigma^2}{\omega_0^2}\frac{d^2}{d\eta^2}+k_\theta^2\rho_i^2s^2\eta^2+\frac{2\varepsilon_n}{\omega_0}\left[\cos(\eta+\theta_0)+s\eta\sin(\eta+\theta_0)\right]+\frac{\omega_0-1}{\omega_0+\eta_i}-k_\theta^2\rho_i^2\right]\xi(\eta,\theta_0)=0 \qquad (3)$$

Note that this involves an arbitrary phase angle, θ_0, which can be interpreted as the poloidal angle about which the mode balloons. θ_0 is often selected to maximise the growth rate, but a more rigorous procedure shows it is usually more complicated than this, as we discuss here.

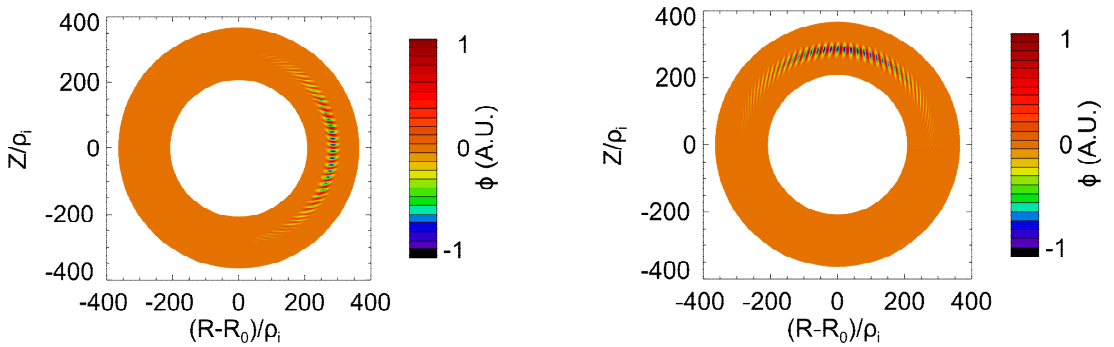

Figure 1: 2D eigenmode in the poloidal cross-section for a case where η_i has a maximum at x=0 (left) and one where η_i is linear in x (right). All other equilibrium variables are equal in both cases.

To illustrate the importance of the correct treatment of the mode structure, we derive two global 2D solutions to Eq (1). In the first, shown in Fig 1 (left), we take all equilibrium parameters to be independent of x except for η_i, for which we adopt a parabolic profile, with a maximum at x=0. We see the characteristic ballooning on the outboard side and find a growth rate, Im(ω)=0.32. For the second, shown in Fig 1 (right), we do not change the value of any of the equilibrium parameters at x=0, but now adopt an η_i profile that is linear in x. We find a different mode structure, localised at the plasma top rather than the outboard side, and it is more stable, with Im(ω)=0.24. The solution to the leading order ballooning Eq (3) at x=0 is identical in both cases, yielding the same $\omega_0(x=0, \theta_0)$. As shown in Fig 2, the x-dependence of $\omega_0(x,\theta_0)$ differs for each case; while this is a higher order effect, it nevertheless has a leading order impact on the eigenmode, and the difference between the two 2D mode structures can be explained in terms of this difference in radial dependence [1], as we now describe.

Rather than use the conventional ballooning transform Eq (2), let us instead use the Fourier-ballooning representation, presented in Ref [4]:

$$\phi(x,\theta) = \int_{-\infty}^{\infty} A(\theta_0)\,\xi(\theta,\theta_0)\exp\left[-inq'x(\theta-\theta_0)\right]d\theta_0 \qquad (4)$$

The amplitude factor $A(\theta_0)$ contains the fast variation with θ_0. Equation (1) is then exactly transformed into the ballooning Eq (3), provided we identify $\eta=\theta-\theta_0$. The eigenvalue condition is $\omega=\omega_0(x,\theta_0)$; transforming this into the Fourier-ballooning space, noting $x\rightarrow(i/nq')(d/d\theta_0)$, yields an equation for $A(\theta_0)$ that can be used in Eq (4) to derive $\phi(x,\theta)$, with ω determined as an eigenvalue of the equation for A. The eigenvalue condition is that A must be periodic in θ_0 for ϕ to be periodic in θ. Treating the case with a maximum in the η_i profile first, the top row of Fig 2 illustrates that the local eigenvalue is of the form $\omega = \bar{\omega}(\theta_0) + (\omega_{xx}/2)x^2$, with $\bar{\omega}(\theta_0) = \bar{\omega}_0(1+\varepsilon\cos\theta_0)$. Anticipating that $A(\theta_0)$ is peaked

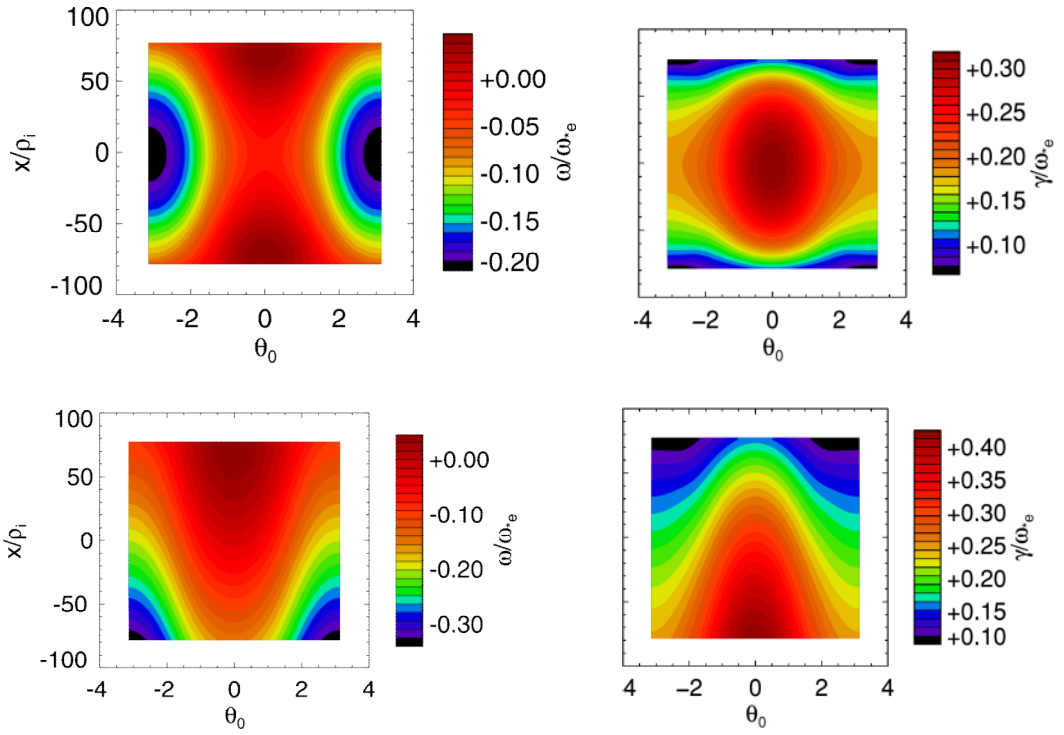

Figure 2: Colour contour plots showing the local ballooning eigenvalue for the peaked η_i case (top) and linear $\eta_i(x)$ case (bottom), for the mode frequency (left) and growth rate (right).

around the stationary point where $\theta_0=0$, we expand the cosine to derive:

$$\frac{\omega_{xx}}{2n^2q'^2}\frac{d^2A}{d\theta_0^2}+\left[\omega-\overline{\omega}_0(1+\varepsilon)-\frac{\omega_{\theta_0\theta_0}}{2}\theta_0^2\right]A=0 \qquad (5)$$

This yields a Gaussian for A, which is indeed strongly peaked around $\theta_0=0$ with a width $\sim n^{-1/2}$. It yields an eigenvalue $\omega=\overline{\omega}(1+\varepsilon)+O(n^{-1})$, so the growth rate is the maximum of $\mathrm{Im}[\omega_0(x,\theta_0)]$ which, from the top right-hand panel of Fig 2 provides $\mathrm{Im}(\omega)=0.32$ in excellent agreement with the 2D result. Because A is peaked around $\theta_0=0$, it projects out $\xi(\theta_0=0,\theta)$ in Eq (4), explaining the outboard ballooning nature. Note that both the local mode frequency *and* the local growth rate must be stationary at the same radial location to expand ω_0 as a quadratic in x. This can only happen at certain discrete positions in the plasma, so this type of mode is termed an *isolated* mode.

More generally we must expand $\omega=\overline{\omega}(\theta_0)+\omega_x x$, and then our eigenmode equation for A is:

$$\frac{i\omega_x(\theta_0)}{nq'}\frac{dA}{d\theta_0}+\left[\omega-\overline{\omega}_0(1+\varepsilon\cos\theta_0)\right]A=0 \qquad (6)$$

Requiring A to be periodic in θ_0 provides an eigenvalue condition $\omega=\langle\overline{\omega}/\omega_x\rangle\langle\omega_x^{-1}\rangle^{-1}$, where angled brackets denote an average over θ_0. Fitting to the lower row of contour plots in Fig 2, ω_x is approximately independent of θ_0, so we find $\mathrm{Im}(\omega)=\mathrm{Im}(\overline{\omega}_0)=0.24$, again in good

agreement with the global calculation. The solution of Eq (6) provides $A = \exp\left[-inq'\left(\overline{\omega}_0 \varepsilon / \omega_x\right)\sin\theta_0\right]$ which is strongly peaked around $\theta_0=\pi/2$. This selects $\theta_0=\pi/2$ in the Fourier-ballooning transform, explaining the localisation at the top of the tokamak.

To illustrate how this model might affect ELM size, consider an EPED-type model [5] where pedestal transport is constrained by a toroidal microinstability (we do not specify which as our model is generic) and its gradient is constrained by ideal MHD. The upper panels of Fig 3 show the situation when the maxima in local frequency and growth rate are not aligned. The stability diagram shows a cartoon for how the marginal stability boundary of the isolated mode might look (but this *is not accessible* to the plasma in these conditions). Only the general mode drives turbulence, which occurs above the upper boundary at high gradient. In a stiff transport model this would constrain the pedestal gradients, but the pedestal can continue to widen until it encounters the ideal MHD stability boundary, when a large type I ELM will be triggered, as illustrated [5]. Under certain conditions, eg a critical flow shear, as the pedestal evolves the plasma may encounter a parameter regime where the isolated mode is allowed as it tracks the general mode stability boundary. This would trigger an isolated mode with a substantial growth rate (i.e. not at the marginal stability boundary), driving a large transport event and a small crash in the pedestal gradients back towards the isolated mode stability boundary, and away from the dangerous ideal MHD boundary. This could provide an interpretation of the replacement of large type I ELMs with smaller ones, with mixed small and large ELMs expected in the transition regime.

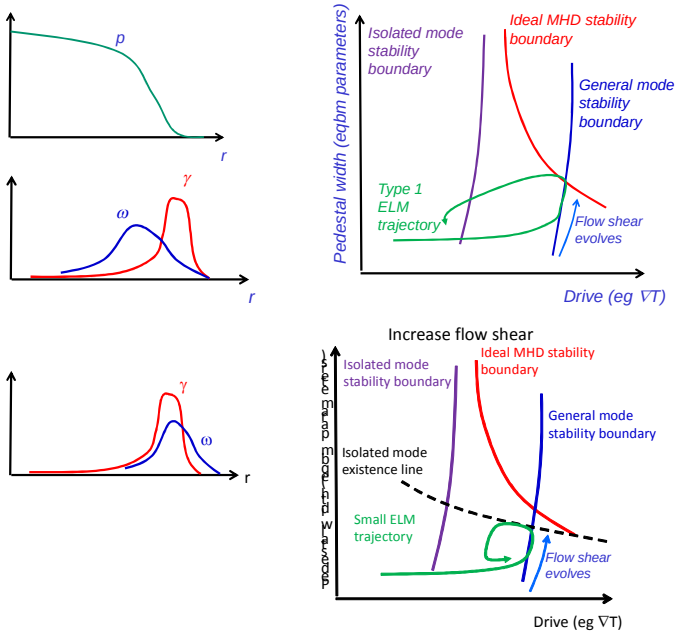

Figure 3: Model pedestal pressure profile and related local mode frequency and growth rates (left) together with stability boundaries and parameter evolution between ELMs for a case when no isolated mode can exist (top) and when an isolated mode can exist along a line of parameter space (bottom). A critical flow shear, for example, can cause the transition from general to isolated modes.

References

[1] J.B. Taylor, H.R. Wilson and J.W. Connor, Plas Phys Cont Fusion **38** (1996) 243A.
[2] J.W. Connor and J.B. Taylor, Phys Plasmas **30** (1987) 3180
[3] J.W. Connor, R.J. Hastie and J.B. Taylor, Proc. Roy. Soc. London Ser. A **365** (1979)
[4] Y.Z. Zhang and S.M. Mahajan, Phys. Lett. **157A** (1991) 133
[5] P.B. Snyder et al, Nucl. Fusion **51** (2011) 1030126